Load Distribution Analysis of Spline Joints

J. Hong, D. Talbot, A. Kahraman

A finite elements-based contact model is developed to predict load distribution along the spline joint interfaces; effects of spline misalignment are investigated along with intentional lead crowning of the contacting surfaces. The effects of manufacturing tooth indexing error on spline load distributions are demonstrated by using the proposed model.

Introduction

Splines are used commonly in power transmission systems for coupling two rotating components such as a shaft and its gear. They provide higher load carrying capacity over keyed shafts, and hence, represent better durability performance. In addition, they can tolerate a certain amount of angular misalignment and relative sliding between their internal and external components. The most common failure modes observed in spline joints include surface wear, fretting corrosion fatigue, and tooth breakage (Refs. 1, 2). In spite of such experimental studies, little is known about spline failure mechanisms since accurate load distribution prediction models are not available, especially for the cases where the loading is three-dimensional as in the case of helical or cross-axis gear splines (Refs. 3–10). These models can predict load distribution of splines, but they are limited to simple loading conditions. Other complicating effects such as spline surface modifications and spline tooth manufacturing errors such as indexing or spacing errors are also not considered in these models.)

This paper aims at developing a finite elements (FE)-based computational model of gear-shaft splines. The objectives of this paper are as follows:

- Develop a computational model of a gear-shaft spline interface under combined torsion, radial forces and tilting moments.
- Establish nominal load distribution conditions under pure torsion, spur gear loading (torsion and radial force) and helical gear (torsion, radial force and tilting moment) loading conditions.
- Quantify the change to baseline load distributions caused by misalignments, spline tooth (lead and profile) modifications and spline helix angle.
- Investigate the influence of indexing errors on baseline spline load distributions.

Computational Model

A commercial FE-based contact mechanics model *Helical-3D* (Advanced Numerical Solutions, Inc.) designed specifically for loaded contact analysis of helical gears is modified here to analyze spline joints. The core contact solver of this software (*CALYX*) is based on a formulation by Vijayakar (Ref. 11), which combines the finite element method and surface integral method to represent the contact bodies, and calculates the load distribution and rigid body displacements by using the linear programming method. Details of the application of *Helical-3D* to analysis can be found in Reference 12. A brief description will be provided here for completeness purposes.

The first phase of contact analysis is to determine the contact zone. *CALYX* estimates the contact zone by using Hertz's model after locating a set of primary contact points on the contacting surfaces and determining relative principal curvatures and directions. For this, two contacting surfaces, Σ_1 and Σ_2, are defined in terms of their curvilinear parameters s and t as $\mathbf{r}_1(s_1,t_1)$ and $\mathbf{r}_2(s_2,t_2)$. The primary contact points are determined and located when $\mathbf{r}_1$ and $\mathbf{r}_2$ become the closest to each other (Ref. 11). For this, the surface $\mathbf{r}_1(s_1,t_1)$ is discretized into a grid of points $\mathbf{r}_{1ij}(s_{1i},t_{1j})$. For each of these grid points, a primary contact point $\mathbf{r}_{2ij}(s_{2i},t_{2j})$ is determined such that $||\mathbf{r}_1(s_1,t_1) - \mathbf{r}_2(s_2,t_2)||$ is minimum. The principal curvatures and principal directions of two surfaces at the common contact point $\mathbf{p}$ are determined in terms of the coefficients of the first and second fundamental form of the surfaces. The second phase is to compute the compliance matrix and set up the contact equation to be solved by a modified simplex method. Hertzian theory is used to predict the size of the contact zone and consequently a grid of points in the contact zone is laid out on both surfaces. Then a surface integral method near the contact zone and a finite element method away from the contact zone are combined to predict cross compliance terms between the set of grid points.

The displacement $u(\mathbf{r}_{ij};\ \mathbf{r})$ at a field point $\mathbf{r}$ caused by a unit normal force at surface grid point $\mathbf{r}_{ij}$ is given as (Ref. 11):

$$u(r_{ij};r) = (u^{(si)}(r_{ij};r) - u^{(si)}(r_{ij};q)) + u^{(fe)}(r_{ij}r;q) \quad (1)$$

Here $\mathbf{q}$ is some location inside the body on a matching surface, sufficiently far beneath the tooth surface. The first two terms in this equation denote the relative deflection of $\mathbf{r}$ with respect to $\mathbf{q}$, which is evaluated using the surface integral formulae. The third term denotes the displacement of $\mathbf{q}$, which is computed using finite element method. The point $\mathbf{q}$ is chosen such that elastic half-space assumption will be valid and the finite element prediction will not be significantly affected by local stresses on the surface. The surface integral and finite element solutions are combined along this matching surface interface, as

This work is the sole property of the Gear and Power Transmission Research Laboratory Department of Mechanical and Aerospace Engineering, The Ohio State University, 201 W. 19th Avenue, Columbus, OH 43210, USA

described in detail (Ref. 11). The combination of surface integral formulae and finite element method described above provides an accurate and numerically efficient way of obtaining the compliance matrix for the contacting bodies.

Finite Element Model of an Example Spline and Analysis Results

Figure 1 shows the contact model for an example clearance-fit spline joint that is designed according to ANSI Standard B92.1-1996; Table 1 lists its main parameters. The system model consists of a shaft, an external spline and an internal spline. Over the potential contact area, the model shown in Figure 1 uses a contact grid with M number of elements in the face width direction and N number of elements along the profile direction. Within each contact element there are two contact grids in both face width and profile direction. Width of the contact cells is defined such that $2N$ grids in the profile direction can capture all the contact on the tooth. With this, a spline joint with Z teeth would have a total of $Z \times 2M \times 2N$ grid cells defining the contacts along the drive flanks of the teeth. The model allows intentional deviations from the involute spline tooth surfaces such as profile and lead modifications as in spur and helical gears to prevent any undesirable edge contact conditions. In addition, a similar contact grid with the same resolution can be defined along the other Z coast tooth surfaces to capture any back side contacts.

This example spline interface is loaded in two different ways. In the first case, a moment (torsion) T is applied to the end of the shaft (Figure 2a), while the cylindrical disk having the internal spline is constrained along its perimeter to represent a purely torsional loading of the spline with no radial force and tilting moment. The second loading case (Figure 2b) represents a spline supporting a gear where T, applied torque, is balanced by (a) the mesh force $F_n = 2T/(d_p \cos\alpha_n)$ where α_n and d_p are the normal pressure angle and pitch circle diameter of the gear, respectively, F_n that is acting on the normal plane of the gear along the line of action has a tangent component $F_t = 2T/d_p$, a radial component $F_r = F_t \tan\alpha_n / \cos\beta$ and an axial component $F_a = F_t \tan\beta$, where α_n, β and d_p are the normal pressure angle, helix angle and pitch circle diameter of the gear, respectively. This results in a torsion T about the rotational axis z of the shaft, radial forces $F_x = F_t$, $F_y = -F_r$, and tilting moment $M_x = T \tan\beta$ about the x axis in Figure 2b. In this case, the moment M_x was applied in addition to F_x and F_y to the gear tooth and T applied to the input end of the shaft.

Influence of loading conditions. In case of pure torsion loading (Figure 2), identical load distributions on each spline tooth are predicted with the load varying in an exponential manner in the face width direction. Figure 3a shows various views of the shaft spline to demonstrate the loads carried by individual contact grid cells on each tooth. As this type of a representation of the tooth load distributions is not practical, the contact surface of each tooth of the shaft spline was mapped to a rectangular window (Figure 3b) with the load distribution of the tooth surface displayed on this window. Using this method, load distributions on all of the teeth can be viewed simultaneously and conveniently (Figure 4) for this torsional loading case. Figure 4 shows the load distributions on the spline teeth under pure torsion at torque levels of $T = 2{,}000$ and $4{,}000$ Nm. For instance, at $T = 4{,}000$ Nm, maximum contact stress is predicted to be about 123 MPa that occurs at the edge on the input side where the torque is applied to the shaft. Contact stresses reduce significantly with the axial distance from this edge. Non-uniform load distributions become clearer with increased T while the location of maximum stress remains at the input-side edge. It is noted that as the torque increases, the contact area extends towards the edge of the spline teeth along the profile direction and the contact stress increases simultaneously — with the load distribution pattern remaining the same.

Table 1 Example spline design used in this study

	External spline	Internal spline
Number of teeth	25	
Spline Module [mm]	3.175	
Pressure angle	30°	
Base diameter [mm]	68.732	
Major diameter [mm]	82.550	85.725
Form diameter [mm]	76.022	82.728
Minor diameter [mm]	73.025	76.200
Circular space width [mm]	-	5.055
Circular tooth thickness [mm]	4.981	-
Inner rim diameter [mm]	58	95
Outer rim diameter [mm]	64	150
Inner shaft diameter [mm]	45	-
Outer shaft diameter [mm]	58	-
Profile crown [µm]	5	0.0

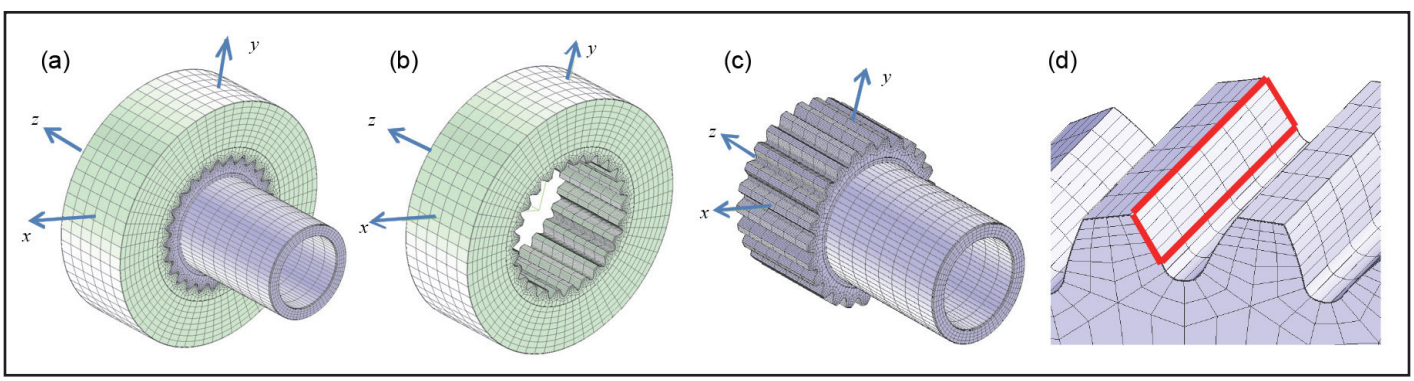

Figure 1 Spline finite element model; (a) spline interface, (b) internal spline, (c) external spline and shaft, (d) potential contact area and contact elements.

Next, consider a helical gear loading case. Relevant helical gear tooth parameters are the normal pressure angle of $\alpha_n = 20°$, and the pitch circle diameter of $d_p = 160$ mm. Helix angle β of the gear is varied from 0° (spur gear loading) to 20° at a torque value of 4,000 Nm to predict the load distributions shown (Figure 5). For the spur gear loading (Figure 5a), load sharing along the face width direction is still biased towards the side where torque is applied. Load distributions are no longer identical for all the spline teeth since the loading is no longer axisymmetric. With tooth #1 centered below (and closest to) the gear mesh, teeth 1-8 and 21-25 are shown to experience larger loads while teeth #9-20 bear less load. For instance, the resultant maximum contact stresses at $T = 4{,}000$ Nm are 129, 108, 101 and 167 MPa for teeth #5, #10, #15 and #24, respectively, as a direct consequence of this unequal loading. In comparison to Figure 5a, helical gear loading maintains the same qualitative load sharing characteristics of spline teeth. Figures 5b and 5c show that teeth #1-8 and #21-25 carry larger load, while teeth #9-20 are loaded less. This can be explained by the fact that the spline interface transmitted the same radial load in spur gear loading and helical gear loading conditions. However, a remarkable difference is observed that axial load distribution on teeth #19-25 and #1-2 is biased to the opposite side to which torque is applied. This is due to the additional tilting moment M_x transmitted over the spline interface, which causes the load on some teeth to be biased to the other side to balance it. It is observed that as β increases, the load on each tooth gets more concentrated on the side where the load is biased. For instance, loads on teeth #3-10 are concentrated to the side where the torque is applied, while loads on teeth #20-25 are concentrated to the opposite side. The maximum contact stresses are 182 and 334 MPa for $\beta = 10°$ and 20°, respectively, with the corresponding tilting moments of $M_x = 705$ and 1,456 Nm. The load concentration increases significantly because of the larger resultant tilting moment on the spline when the β increases.

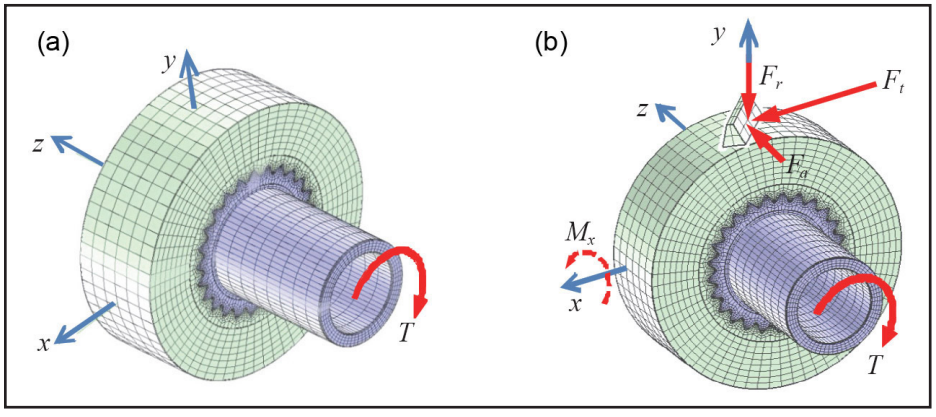

Figure 2 A spline model with different loading conditions; (a) pure torsion loading and (b) gear loading.

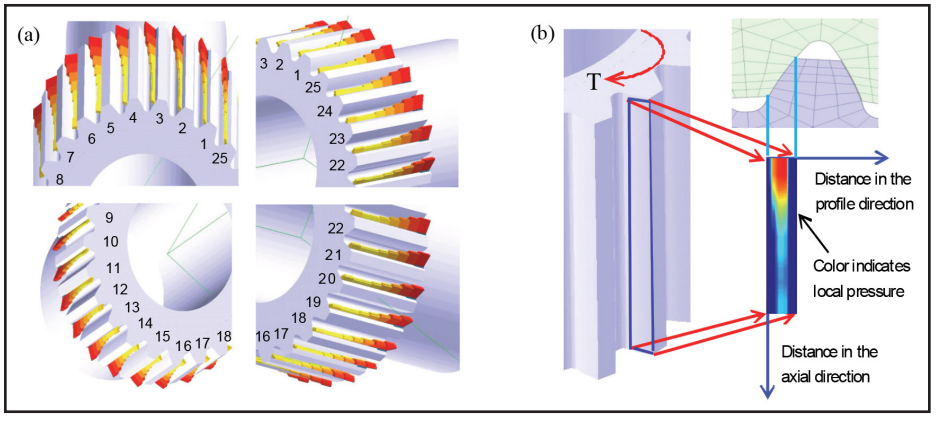

Figure 3 (a) Load distribution of a spline under pure torsion loading, and (b) mapping of the load distribution on a tooth to a rectangular window.

Effect of Design Variations

Misalignments and lead crown modifications. Misalignment of spline couplings has been recognized as harmful to splines because it causes significant load concentration on spline teeth, and accelerates wear and fretting fatigue of splines (Refs. 2, 13). Significant load concentration observed in both misaligned splines (Figure 6a, a misalignment of $\varphi = 0.12°$) and splines experiencing helical gear loading (Figure 5b-c) can be potentially remedied by applying a lead crown modification along the face width direction. Figure 6 shows load distributions of a spline having a misalignment of $\varphi = 0.12°$ along with different lead crown modifi-

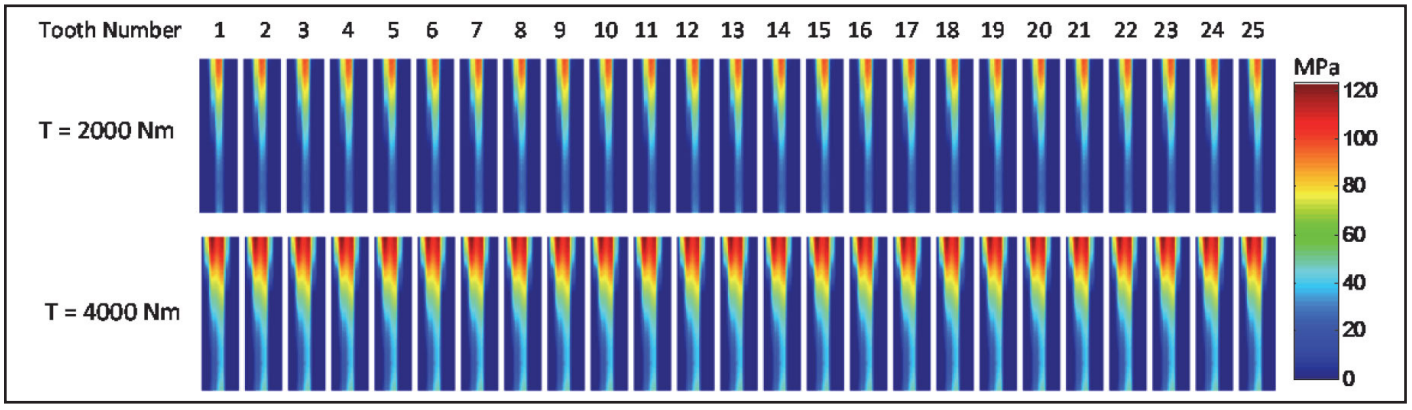

Figure 4 Load distributions of the example spline under pure torsion loading at different torque levels.

cation magnitudes of $\delta = 0$ and 40 μm at $T = 4{,}000$ Nm under pure torsion loading. It is observed that the crown modification moves the load from the edge to the center of the spline, in the process reducing the maximum contact stresses significantly. Figure 7 shows load distributions on the splines with different lead crown modification magnitudes of $\delta = 0$ and 40 μm for helical gear loading with $\beta = 20°$ at $T = 4{,}000$ Nm. Unlike in the misaligned spline case, lead crown modification under a helical gear loading condition neither reduces load concentration, nor moves the tooth load from the edge to the center. This occurs because the moment acting on the spline remains a constant for a given torque in helical gear loading despite the lead crown modification. The biased load concentration exists no matter how much lead crown modification is adopted.

***Helical splines*:** Figure 8 shows the load distributions of helical splines having different spline helix angles of $\gamma = -10°$, 0° and 10° under helical gear loading condition with a helical gear ($\beta = 20°$) at $T = 4{,}000$ Nm . A negative spline helix angle represents a left-handed helix and a positive helix angle represents a right-handed helix. It is observed that a right-hand spline helix helps reduce load concentration, and a left-hand spline helix condenses the load concentration. For instance, the maximum contact stresses are 334 MPa for a spur spline ($\gamma = 0°$) under helical gear loading with a right-hand helical gear. The maximum contact stress increases dramatically to 754 MPa for left-hand spline helix angles of $\gamma = -10°$. On the other hand, the maximum contact stresses drop significantly to 211 MPa for right-handed splines with helix angles $\gamma = 10°$. The maximum contact stress is reduced by more than 35% and more teeth are observed to carry load (Figure 8c). The dominant factor is that the spline helix introduces an axial load that can either increase the tilting moment or counterbalance the tilting moment, depending on its direction. For a spline loaded by a right-handed gear, a right-hand spline helix would induce an axial load to counterbalance the tilting moment thus reducing the load concentration. On the other hand, a left-hand spline helix would induce an axial load, which would increase the tilting

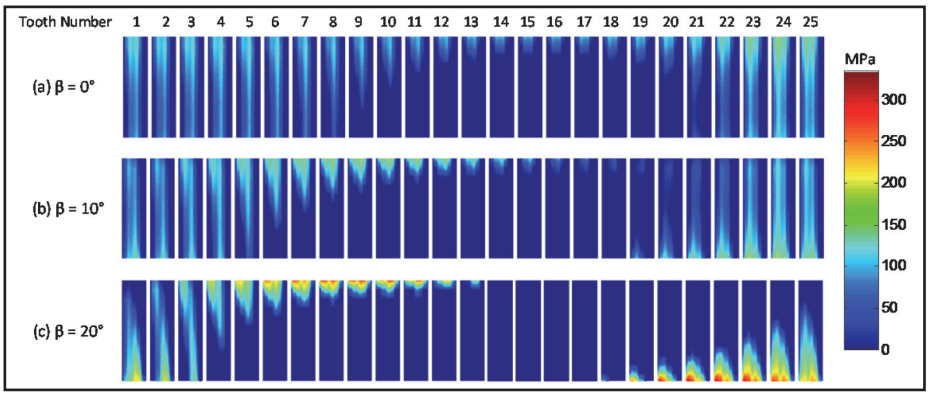

Figure 5 Load distributions of a spline under helical gear loading with different helix angles, β, at T = 4,000 Nm.

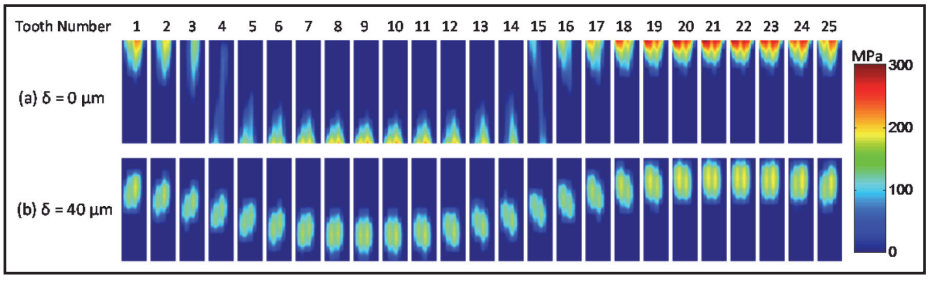

Figure 6 Load distributions of a misaligned spline having different lead crown modification magnitudes, δ, at T = 4,000 Nm and φ = 0.12°.

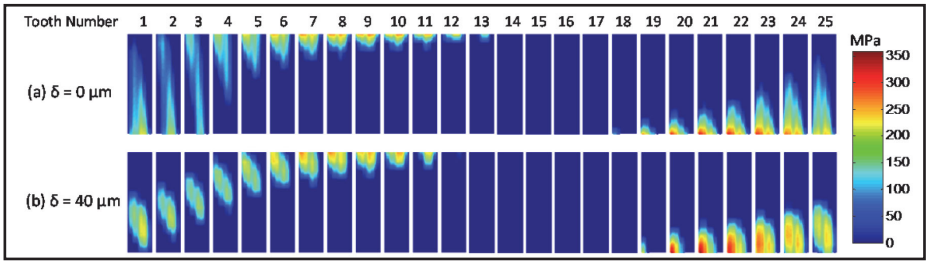

Figure 7 Load distributions of a spline under helical gear loading having different lead crown modification magnitudes, δ, at T = 4,000 Nm, and β = 20°.

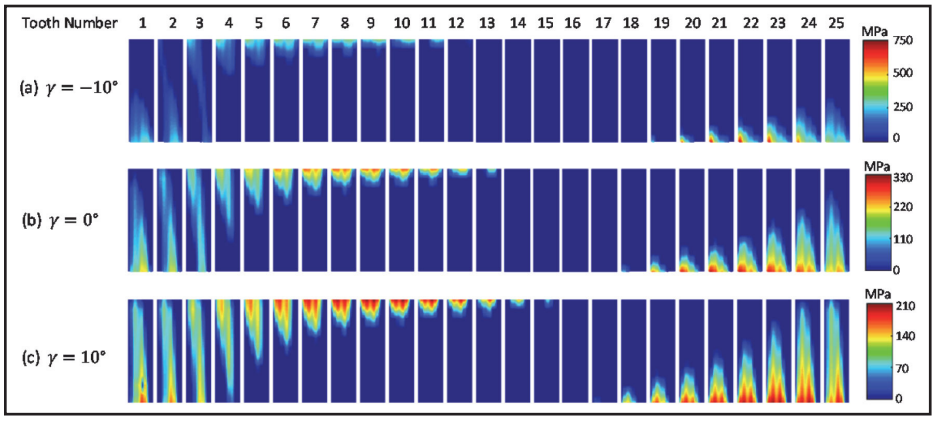

Figure 8 Load distributions of helical splines having different spline helix angles, γ, under helical gear loading with a gear helix angle, β = 20°, at *T* = 4,000 Nm.

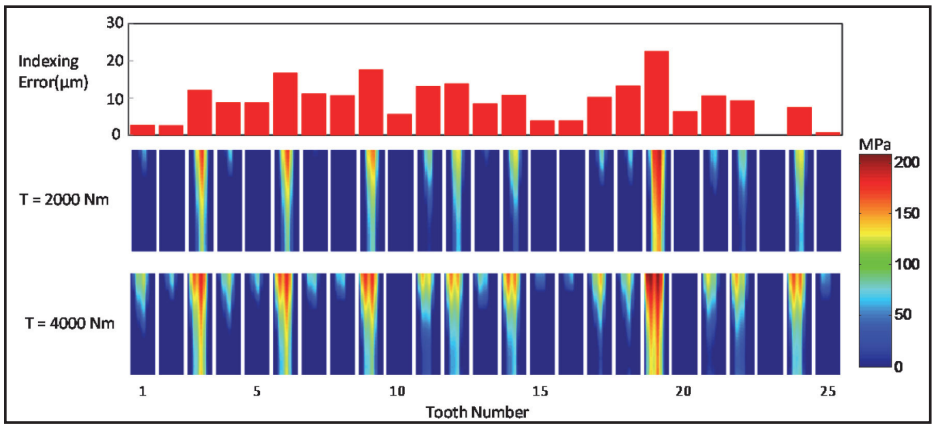

Figure 9 Load distributions of a spline having random tooth indexing errors at different torque levels.

moment thus resulting in larger load concentration on the spline teeth. The result implies that in helical gear loading conditions, selecting a helical spline with the same helix direction as that of the helical gear could reduce the load concentration, and improve load distribution.

Effect of Spline Tooth Indexing Errors

Investigations of spline load distributions discussed above all assumed perfect tooth geometry, ignoring the effect of tooth indexing errors. However, it occurs frequently that some spline teeth exhibit heavier damage than others, which might be caused by spline tooth indexing errors (Refs. 12-14). In order to demonstrate the effect of indexing errors on spline load distributions, a spline joint with a random tooth indexing error distribution is considered next. Figure 9 shows a random tooth indexing error sequence considered together with the corresponding spline load distribution at $T = 2{,}000$ and 4,000 Nm under pure torsion condition. Load concentrations are observed on spline teeth having larger indexing error, such as spline tooth #6, #9, #12 and #19. Teeth with larger indexing error have smaller clearance, and they will engage first. Teeth with smaller indexing error have larger clearance and they will gradually come into contact when the torque increases to a certain level. Figure 9 emphasizes that the load concentration resulting from spline tooth indexing error is significant and must be accounted for in the design of a spline at a certain quality level.

Summary and Conclusions

A finite element-based computational model of a gear spline-shaft interface under combined torsional load, radial load and tilting moment was proposed. Load distributions of the baseline system of the spline coupling under pure torsion, spur gear loading and helical gear loading were characterized. Pure torsion loading results showed identical load distributions on all spline teeth, with each tooth exhibiting exponentially decreasing load in axial direction while helical gear loading led to cyclic load concentration oscillating across the face width of the spline teeth. The effectiveness of lead crown in improving load distributions of misaligned splines was demonstrated. Selecting a helical spline with the same helix direction as that of the helical gear loading the spline was shown to reduce the load concentration and improve load distribution of splines undergoing helical gear loading. Finally, effects of indexing errors of spline teeth were investigated for the pure torsion loading case to show significant unequal load sharing at spline teeth due to indexing errors.

Acknowledgement. *The authors thank Dr. Sandeep Vijayakar of Advanced Numerical Solutions, Inc. for making* Helical-3D *available.*

References

1. Ku, P.M. and M.L. Valtierra. "Splice Wear Effects of Design and Lubrication," *J. Eng. for Ind.*, 97 (1975) 1257-1263.
2. Brown, H.W. "A Reliable Spline Coupling," *J. Eng. for Ind.*, 101 (1979) 421-426.
3. Volfson, B.P. "Stress Sources and Critical Stress Combinations for Splined Shaft," *J. Mech. Des.*, 104 (1982) 551-556.
4. Barrot, A., M. Paredes and M. Sartor. "Determining Both Radial Pressure Distribution and Torsional Stiffness of Involute Spline Couplings," *Proc. IMechE*, Part C: 220 (2006) 1727-1738.
5. Limmer, L., D. Nowell and D.A. Hills. "A Combined Testing and Modeling Approach to the Prediction of the Fretting Fatigue Performance of Splined Shafts," *Proc. Instn. Mech. Engrs.*, Part G, 215 (2001) 105-112.
6. Kahn-Jetter, Z. and S. Wright. "Finite Element Analysis of an Involute Spline," *J. Mech. Des.*, 122 (2000) 239-244.
7. Tjernberg, A. "Load Distribution in the Axial Direction in a Spline Coupling," *Engineering Failure Analysis*, 8 (2000) 557-570.
8. Leen, S.B., I.J. Richardson, I.R. McColl, E.J. Williams and T.R. Hyde. "Macroscopic Fretting Variables in a Splined Coupling under Combined Torque and Axial Load," J. Strain Analysis 36 (2001) 481-497.
9. Adey, R.A., J. Baynham and J.W. Taylor. "Development of Analysis Tools for Spline Couplings," *Proc. Instn. Mech. Engrs.*, Part G, 214 (2000) 347-357.
10. Medina, S. and A.V. Olver. "Regimes of Contact in Spline Coupling," *J. of Trib.*124 (2002) 351-357.
11. Vijayakar, S. "A Combined Surface Integral and Finite Element Solution for a Three-Dimensional Contact Problem," Int. J. for Numerical Methods in Engineering 31 (1991) 525-545.
12. Hong, J., D. Talbot and A. Kahraman. "Load Distribution Analysis of Clearance-fit Spine Joints using Finite Elements," *Mechanisms and Machine Theory*, 74 (2014) 42-57.
13. Medina, S. and A.V. Olver. "An Analysis of Misaligned Spline Coupling,"*Proc. Instn. Mech. Engrs.*, Part J, 216 (2002) 269-279.
14. Chase, K.W., C.D. Sorensen and B.J.K. DeCaires."Variation Analysis of Tooth Engagement and Loads in Involute Splines," *IEEE Trans. Autom. Sci. Eng.* 7 (2010) 54-62.

For Related Articles Search
splines
at www.geartechnology.com

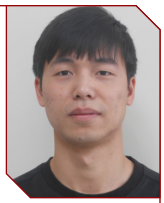

Jiazheng Hong is a Ph.D. student at Mechanical and Aerospace Engineering at the Ohio State University. He conducts research projects in gear and spline contact mechanics for Gear and Power Transmission Research Laboratory.

David Talbot is a Research Scientist at Mechanical and Aerospace Engineering at the Ohio State University. He is specialized in gear system efficiency, gear manufacturing and geometry and load distribution simulation.

Ahmet Kahraman is a Professor of Mechanical and Aerospace Engineering at the Ohio State University. He is the Director of Gleason Gear and Power Transmission Research Laboratory. He also directs Pratt & Whitney Center of Excellence in Gearbox Technology.